Modeling of dynamics of nanosecond laser ablation in phase explosion regime

Conference Paper · August 2017

DOI: 10.1117/12.2271981

4 authors:

Vladimir I. Mazhukin
Russian Academy of Sciences
207 PUBLICATIONS **1,273** CITATIONS
SEE PROFILE

A. V. Shapranov
Keldysh Institute of Applied Mathematics
48 PUBLICATIONS **264** CITATIONS
SEE PROFILE

Michael Demin
41 PUBLICATIONS **206** CITATIONS
SEE PROFILE

Alexander V. Mazhukin
Russian Academy of Sciences
37 PUBLICATIONS **220** CITATIONS
SEE PROFILE

PROCEEDINGS OF SPIE

SPIEDigitalLibrary.org/conference-proceedings-of-spie

Modeling of dynamics of nanosecond laser ablation in phase explosion regime

V. I. Mazhukin
A. V. Shapranov
M. M. Demin
A. V. Mazhukin

SPIE.

Modeling of dynamics of nanosecond laser ablation in phase explosion regime.

V. I. Mazhukin[a,b], A.V.Shapranov[a,b], M.M.Demin[a], A.V. Mazhukin[a,b]
[a]Keldysh Institute of Applied Mathematics, Russian Academy of Sciences, Miusskaya pl. 4, Moscow, 125047 Russia; e-mail: vim@modhef.ru
[b]National Research Nuclear University "MEPhI", Kashirskoe sh. 31, Moscow, 115409 Russia

ABSTRACT

A hydrodynamic model was developed that takes into account the kinetics of heterogeneous phase transitions (melting and evaporation) under the action of pulsed laser radiation on metal targets. With the use of continual and molecular dynamic modeling, the initial stage of the explosive boiling of an Al target under the influence of ns laser radiation was studied. The simulation confirmed the presence of a temperature maximum below the surface of superheated metastable liquid underlying the homogeneous evaporation (phase explosion) of metals.

Keywords: pulsed laser ablation, hydrodynamic and atomistic models, explosive boiling, heterogeneous phase transitions, molecular dynamics simulation.

1. INTRODUCTION

The continuing interest in pulsed laser ablation (PLA)[1-5] is primarily due to the increasing possibilities of its use in many applications: micromachining[6], laser-induced breakdown spectroscopy (LIBS)[7,8] surface micro-nano-structuring[9], biomedicine[10,11].

Laser irradiation of solid targets with short nanosecond pulses initiates a complex sequence of processes that occur during and after the laser exposure. Earlier, the effect of nanosecond laser pulses on metals was studied in a number of experimental and theoretical studies[12-15]. However, a number of important physical processes underlying ablation are still poorly understood due to their complexity. The presence of a large number of interrelated physical processes makes it difficult to experimentally determine and study the basic mechanisms of ablation. The most complex of these are homogeneous phase transitions in the vicinity of the critical point[16-18]. For this reason, nanosecond laser ablation continues to be an active research area in which mathematical modeling plays an increasing role[19,20]

In this paper, we consider the continuum and atomistic approaches to the theoretical study of the dynamics of heterogeneous (melting, evaporation) and homogeneous (explosive boiling) phase transitions in an aluminum target under the influence of ns-laser pulses with duration of $\tau = 3\,ns$, fluence $F = 5.2 J/cm^2$ and wavelength $\lambda = 1.06 \mu m$.

For the theoretical description and analysis of the PLA process of condensed media, various theoretical approaches are used: continuum, kinetic, atomistic (molecular dynamical, etc.) Each of them has its own field of applicability, its advantages and disadvantages.

2. CONTINUUM APPROACH. MATHEMATICAL MODELS.

The most common is the continuum approach, using the concepts and equations of continuum mechanics with the necessary boundary conditions on the existing or emerging interface surfaces of matter with different phase states.

Within the continuum approach, the mathematical description of the PLA processes is realized, as a rule, in the form of hydrodynamic models that take into account the reaction of the irradiated material to varying density, pressure, and energy, both in the target and in the vapor-gas medium. Simpler thermal models are also widespread, in which only the temperature fields are taken into account. The greatest difficulty in the continuum approach is the description of the homogeneous mechanisms of phase transformations: melting - crystallization and evaporation.

The success of theoretical studies using mathematical modeling largely depends on the successful selection of adequate mathematical models and numerical methods for their solution. As an example of the difficulties with the use of mathematical models, it is possible to indicate a wide application of equilibrium equations of state for the description of heterogeneous mechanisms of fast phase transitions. The use of the equations of state greatly simplifies the computational algorithm, since it allows us to exclude moving interphase boundaries from consideration, but information about the nonequilibrium metastable (superheated / undercooled) states of matter is lost.

Third International Conference on Applications of Optics and Photonics, edited by Manuel F. M. Costa,
Proc. of SPIE Vol. 10453, 104530X · © 2017 SPIE · CCC code: 0277-786X/17/$18 · doi: 10.1117/12.2271981

Also, the difficulties associated with understanding of the mechanism of homogeneous phase transitions in metals occurring under the action of ns-laser pulses are also known. In dielectrics[21,22] and weakly absorbing liquids[23] exposed to laser irradiation, the mechanism of explosive boiling is associated with the appearance of a temperature maximum below the surface of the substance. The validity of this statement was confirmed by the results of an analytical[21] and numerical[22, 23] solution of the thermal model. However, for strongly absorbing media, mainly metallic, calculations based on the thermal model[22-26] have shown that the magnitude of the near-surface temperature maximum is several degrees. In view of its smallness, the overheating was excluded from consideration, and explosive boiling was treated as a surface spattering of the liquid phase when a critical temperature is reached at the surface[27]. This interpretation is not convincing, since it does not allow to determine, even approximately, the parameters of explosive boiling. The fundamental reason for the discrepancy between modeling results is the impossibility of taking into account, within the framework of the thermal model, of strong changes in the thermo-physical and mechanical characteristics of the substance in the metastable state in the vicinity of the critical point. Available hydrodynamic models are free from these shortcomings that make it possible to describe the processes of surface evaporation up to the transition to the supercritical regime expansion of matter.

2.1 The hydrodynamic model

Most PLA applications are performed in the presence of ambient gas, which leads to the need to consider laser heating, melting and evaporation of the Al target in a medium with back pressure (air). Air, for the selected exposure mode, is completely transparent to laser radiation, which is partially reflected from the metal surface, and partially absorbed by the target material layer. The energy release of the laser pulse is of volume nature. As the interior of the target is warmed, the melting front $\Gamma_{s\ell}(t)$ runs from its surface forming a new region of the liquid phase. Further heating leads to the appearance of a front of heterogeneous evaporation $\Gamma_{\ell\upsilon}(t)$ that runs inside the melt. On the surface of the melt, a stream of evaporated matter is formed, which pushes out air and forms another new phase - vapor. The new area occupied by the vapor is limited on one side by a moving interface (evaporating surface) $\Gamma_{\ell\upsilon}(t)$, and on the other by a movable contact boundary of the vapor-air $\Gamma_{\upsilon g}(t)$. To describe the behavior of each of the four media, the system of equations of hydrodynamics supplemented by the equations of energy, the transfer of laser radiation, and the corresponding equations of state was used. At the interfaces of the media, the equation of hydrodynamics are linked by the appropriate boundary conditions.

$$\left[\begin{array}{l} \dfrac{\partial \rho}{\partial t}+\dfrac{\partial(\rho u)}{\partial x}=0, \\ \dfrac{\partial(\rho u)}{\partial t}+\dfrac{\partial\left(\rho u^{2}\right)}{\partial x}+\dfrac{\partial P}{\partial x}=0, \\ \dfrac{\partial(\rho \varepsilon)}{\partial t}+\dfrac{\partial(\rho u \varepsilon)}{\partial x}=-\left(P \dfrac{\partial u}{\partial x}+\dfrac{\partial W_{T}}{\partial x}+\dfrac{\partial G}{\partial x}\right), \\ \dfrac{\partial G}{\partial x}+\kappa_{L}(\rho, T) G=0, \\ W_{T}=-\lambda(T) \dfrac{\partial T}{\partial x} \\ P=P(\rho, T), \quad \varepsilon=\varepsilon(\rho, T) \end{array}\right]_{k} \quad k=s, l, \upsilon, g \qquad (1)$$

$$t>0, \qquad \Gamma_{s}<x<\Gamma_{s\ell}(t)<x<\Gamma_{\ell v}(t)<\Gamma_{vg}(t)<\Gamma_{g}(t)$$

Here $\rho, u, \varepsilon, T, P$ are the density, gas-dynamic velocity, internal energy, temperature and pressure of the substance, respectively, κ_L and G are the absorption coefficient and flux density of laser radiation, W_T is the heat flux density, λ is the thermal conductivity coefficient. The indexes s, l, υ, g denote solid, liquid, vapor and gas (air) phases. In the condensed phase, ε_k has the meaning of the enthalpy of the liquid phase H_k.

2.2 Boundary conditions.

2.2.1. Left fixed boundary, $x = \Gamma_s$**.** As the boundary conditions on the left fixed boundary Γ_s, the condition that the mass and heat flux be zero is used

$$x = \Gamma_s: \qquad u = 0, \quad W_T = 0; \tag{2}$$

2.2.2 Model of heterogeneous (surface) melting - crystallization, $x = \Gamma_{s\ell}$**.**

For fast phase transitions, the heterogeneous melting model consists of a system of equations expressing three conservation laws: mass, momentum and energy, supplemented by the kinetic condition for the velocity of motion of the melting front $\upsilon_{s\ell}$ [28], obtained from the molecular-kinetic theory[29] and which is the main characteristic of the melting-crystallization process. In a stationary (laboratory) coordinate system, the surface melting-crystallization model written on the moving interface of melting $x = \Gamma_{s\ell}(t)$ can be represented in the following form:

$$x = \Gamma_{s\ell}(t): \qquad \rho_s(u_s - \upsilon_{s\ell}) = \rho_\ell(u_\ell - \upsilon_{s\ell})$$

$$p_s + \rho_s(u_s - \upsilon_{s\ell})^2 = p_\ell + \rho_\ell(u_\ell - \upsilon_{s\ell})^2 \tag{3}$$

$$\left(\lambda(T)\frac{\partial T}{\partial x}\right)_s - \left(\lambda(T)\frac{\partial T}{\partial x}\right)_\ell = \rho_s L_m^{ne}\upsilon_{s\ell}$$

$$\upsilon_{s\ell}(\Delta T_{s\ell}) = \alpha\left(3k_B T_{s\ell}/m\right)^{1/2}\left(1 - \exp\left(\beta\frac{L_m(T_m)\mu}{RT_m(P_s)}\frac{\Delta T_{s\ell}}{T_{s\ell}}\right)\right) \tag{4}$$

where α, β are the parameters determined from molecular-dynamic modeling,[30] $\Delta C_{ps} = (C_{ps} - C_{p\ell})$, $\Delta T_{s\ell} = T_{s\ell} - T_m(p_s)$, $T_m(p_s) = T_{m,0} + \alpha p_s$ is the equilibrium melting curve, $L_m(T_m(p_s)) = L_{m0} + \beta\cdot\left(T_m(p_s) - T_{m0}\right)$ is the temperature dependence of equilibrium melting heat [31],

$L_m^{ne} = L_m(T_m(p_s)) + \Delta C_{ps}\Delta T_{s\ell} + \dfrac{\rho_s + \rho_\ell}{\rho_s - \rho_\ell}\dfrac{(u_s - u_\ell)^2}{2}$ is the non-equilibrium melting heat.

2.2.3 The model of heterogeneous (surface) evaporation, $x = \Gamma_{\ell\vartheta}$**.** The surface evaporation process in the Knudsen layer approximation is described by three conservation laws and three additional parameters on the outside of the Knudsen layer: temperature T_υ, density ρ_υ and velocity u:

$$x = \Gamma_{l\upsilon}: \; j_{\ell\upsilon}^m = \rho_\ell\left(u_\ell - \upsilon_{\ell\upsilon}\right) = \rho_\upsilon\left(u_\upsilon - \upsilon_{\ell\upsilon}\right),$$

$$j_{\ell\upsilon}^i = p_\ell + j_{\ell\upsilon}^m\left(u_\ell - \upsilon_{\ell\upsilon}\right) = p_\upsilon + j_{\ell\upsilon}^m\left(u_\upsilon - \upsilon_{\ell\upsilon}\right) \tag{5}$$

$$j_{\ell\upsilon}^e = -j_\ell^T + j_{\ell\upsilon}^m\left[H_\ell + \frac{\left(u_\ell - \upsilon_{\ell\upsilon}\right)^2}{2}\right] - \sigma T_\ell^4 = -j_\upsilon^T + j_{\ell\upsilon}^m\left[H_\upsilon + \frac{\left(u_\upsilon - \upsilon_{\ell\upsilon}\right)^2}{2}\right],$$

where $j_\ell^T = W_\ell = -\lambda\left(T_\ell\right)\dfrac{\partial T_\ell}{\partial x}$, $j_\upsilon^T = W_\upsilon = -\lambda\left(T_\upsilon\right)\dfrac{\partial T_\upsilon}{\partial x}$. With these expressions taken into account, the energy conservation law can be represented in the form:

$$W_\ell - W_\upsilon = \rho_\ell\upsilon_{\ell\upsilon}L_\upsilon^{ne} + \sigma T_\ell^4, \tag{6}$$

$$G\left(\Gamma_{\ell\upsilon}\right) = \left(1 - R(T_\ell)\right)G_0\exp\left(-\left(\frac{t}{\tau}\right)^2\right)$$

where $L_\upsilon^{ne} = L_\upsilon^e\left(T_\ell\right) + C_{p\upsilon}\left(T_b - T_\ell\right) + \dfrac{\rho_\ell + \rho_\upsilon}{\rho_\ell - \rho_\upsilon}\dfrac{\left(u_\ell - u_\upsilon\right)^2}{2}$ is the non-equilibrium heat of evaporation, $R(T_\ell)$ is the reflectivity of target surface, T_b is the boiling temperature, σ is the constant of Stefan-Boltzmann law.

Of the three parameters on the outer side of the Knudsen layer, two of them, usually T_υ and ρ_υ, in general, are determined from the solution of the Boltzmann equation, and the third - the Mach number $M = u/u_c$ - from the solution

of the equations of gas dynamics. As a rule, the Boltzmann kinetic equation is not used directly for determination of T_υ and ρ_υ, and its solution is found using some approximation relations.

In the present work the values of $T_\upsilon, \rho_\upsilon, p_\upsilon$ were determined from the modified Crout model [32]. The modified Crout model is different from similar Knight model[33] in that in the Crout[34] model, the fluxes of mass, momentum and energy has an extremum in $M = 1$:

$$T_\upsilon = \alpha_T(M) T_\ell, \quad \rho_\upsilon = \alpha_\rho(M)\rho_{sat}, \tag{7}$$

where $\alpha_T(M) = \dfrac{2\gamma M^2\left(m^2+0.5\right)^2}{\left(1+\gamma M^2\right)^2 m^2 t^2}$, $\alpha_\rho(M) = \dfrac{1}{\exp\left(-m^2\right)+\pi^{1/2} m\left(1+\mathrm{erf}\left(m\right)\right)} \cdot \dfrac{\left(1+\gamma M^2\right)m^2}{\gamma M^2\left(m^2+0.5\right)^2}$,

The value of m is determined from the equation $F(M)\left(m^2+0.5\right)^2 - m^2\left(m^2+1.5+a\right) = 0,$

where - $F(M) = 1+\dfrac{3\gamma M^2-1}{\left(\gamma M^2-1\right)^2}, \quad a = 2t^2 - 0.5\pi^{1/2} mt - 1, \quad t = \dfrac{2m}{\pi^{1/2}} + \dfrac{1+\mathrm{erf}\left(m\right)}{\exp\left(-m^2\right)+\pi^{1/2} m\left(1+\mathrm{erf}\left(m\right)\right)}$

ρ_{sat} is the density of saturated vapor, $u_c = \sqrt{\gamma RT}$ is the speed of sound, $M = u/u_c$ is the Mach number.

2.2.4 Moving contact boundary, $x = \Gamma_{\upsilon g}(t)$**.** At the contact boundary vapor-air $\Gamma_{\upsilon g}(t)$, the conditions for the continuity of density, pressure, and temperature were formulated:

$$x = \Gamma_{\upsilon g}: \qquad u_\upsilon = u_g,\ P_\upsilon = P_g,\ T_\upsilon = T_g. \tag{8}$$

2.2.5 Moving shock wave, $x = \Gamma_{sh,s}(t)$. The shockwave in air $\Gamma_{sh,g}(t)$ is a strong nonstationary discontinuity, on which three conservation laws are written in the laboratory coordinate system:

$$\begin{aligned} j^m_{sh,g} &= \rho_1(u_1 - \upsilon_{sh,g}) = \rho_0(u_0 - \upsilon_{sh,g}), \\ j^i_{sh,g} &= p_1 + \rho_1(u_1 - \upsilon_{sh,g})^2 = P_0 + \rho_0(u_0 - \upsilon_{sh,g})^2, \\ j^m_{sh,g}&\left(\varepsilon_1 + \frac{(u_1 - \upsilon_{sh,g})^2}{2}\right) - W_{T,1} = j^m_{sh,g}\left(\varepsilon_0 + \frac{(u_0 - \upsilon_{sh,g})^2}{2}\right) - W_{T,0} \end{aligned} \tag{9}$$

Here indexes 0 and 1 denote the values of the quantities on the side of the background and the shock wave, respectively.

2.2.6 Right moving boundary, $x = \Gamma_s(t)$**.** The right boundary on the side of the unperturbed gas is declared moving in order to improve the economics of the computational algorithm. The speed of its motion is found from the differential momentum equation.

2.3 Computational algorithm.

The differential model (1) - (8) was approximated by a family of conservative finite difference schemes written on computational grids with dynamic adaptation[35,36]. The method is based on the idea of transition to an arbitrary nonstationary coordinate system that allows calculations with an arbitrary number of discontinuous solutions, such as shock waves, propagating phase and temperature fronts, contact boundaries and fragmented fragments.

3. RESULTS AND DISCUSSIONS.

The surface of Al target is irradiated by a laser with wavelength $\lambda_L = 1.06\,\mu m$, Gaussian temporal profile $G = G_0 \exp(-(t/\tau)^2)$, with duration $\tau = 3\times10^{-9}$ s, where $G_0 = 9.78\times10^9\ Wcm^{-2}$ is the peak intensity at $t = 0$. The metal surface partially reflects the laser radiation, the rest of the radiation is absorbed by the free electrons of the target. The temperature dependences of the reflectivity of the surface $R(T)$ and the volume absorption coefficient $\alpha(T)$ have the form[37]: $R(T) = R_0 - R_1 T$, $\alpha(T) = \alpha_0 \exp(C_0) - C_1 T + C_2 T^2$. The calculation starts at $t_0 = -4\tau$. The results of the

calculations are compared with the parameters of the critical point of aluminum: $T_c = 7\,600\ K$, $\rho = 0.47\ g/cm^3$, $\rho = 1.42\ kbar$ [38].

The temporal evolution of the processes on the surface of the target is shown in Figs. 1-4. Analysis of time dependencies indicates that the main phenomena, such as the appearance of phase fronts (melting, evaporation), the contact boundary and the shock wave, and the formation of new phase media (liquid, vapor) associated with them occur at the leading edge of the laser pulse. All the processes in the target occur under subcritical conditions, since the maximum value of the surface temperature is $T_{s,\max} \cong 6780\,K$, fig.1, and for the whole temperature profile $T_s(t) < T_c$. Melting starts at $t = -3.9\times10^{-9}\,s$ and is characterized by a kink at the curve $T_s(t)$. The process continues for more than $t > 10^{-8}\,s$, fig. 2. The maximum speed of the melting front is $\upsilon_{s\ell} = 130\ m\,s^{-1}$. During the considered time $t = \left(-3.9\times10^{-9} \div 10^{-8}\right) s$ the produced liquid layer thickness is $\delta_\ell \cong 0.9\mu m$.

The surface evaporation process is illustrated by the relationship of the curves $T_s(t)$ и $T_v(t)$ at fig.1, and by the sign and value of Mach number $\grave{I}\ (t)$. Surface evaporation starts at $t = -2.3\times10^{-9}\,s$, when the saturated vapor pressure begins to exceed the external gas pressure $p_{sat}(t) > p_g(t)$. The temperature on the outside of the Knudsen layer is less than the surface temperature $T_s(t) > T_v(t)$, fig.1, and the Mach number throughout the process differs from zero, but does not exceed 1, $0 < \grave{I}\ (t) \le 1$, fig.2. The evaporation process ceases at $t \approx 6\times10^{-9}\,s$ in the conditions when the laser pulse is almost complete. The termination is characterized by equality $\grave{I}\ (t) = 0$, corresponding to the phase equilibrium, which is replaced by the process of condensation of the evaporated substance on the surface of the target with the inverse relationship between pressure and temperature $p_{sat}(t) < p_g(t)$, $T_s(t) < T_v(t)$ and negative Mach number $\grave{I}\ (t) < 0$. The maximum speed of evaporation front $\upsilon_{\ell\upsilon} = 88\ m\,s^{-1}$ is by 1,5 times lower than that of the melting front. The thickness of the removed layer of matter during the period of surface evaporation $t = \left(-2.3\times10^{-9} \div 6\times10^{-9}\right) s$ is $\delta_\ell \cong 0.09\mu m$.

At the beginning of the evaporation process, the flow of the evaporated substance acting as a piston pushes out the cold air and, performing a certain work, warms up at the peak intensity $G(t=0)$ to a temperature $T_{\upsilon ap} = 4.7\times10^3\,K$ fig. 5 (a). Under the pushing action of the vapor stream, compression of cold dense air occurs, which, after a time, is converted into a shock wave at $t = -2.1\times10^{-9}\ s$. At the time of $t = 0$, the shock wave moves with the speed $\upsilon_{sh,g} = 2.9\ km\,s^{-1}$ and has the temperature $T_{sh,g} = 4.4\times10^3\,K$, ahead of the contact boundary moving with speed $\upsilon_{sh,g} = 2.5\ km\,s^{-1}$ towards the laser beam, fig.5 (a). The temperatures of vapor and air are, in this case, insufficient for the initiation of ionization, and the vapor-gas medium remains transparent for laser radiation.

Figs. 5-7 show spatial distributions of temperature, density, velocity and pressure in the vapor-gas medium at $t = 0$. The most informative is the temperature distribution $T(x)$. From this distribution it follows that the highest temperature is in the near-surface region of the liquid phase bounded from the right by the surface evaporation front $\Gamma_{\ell\upsilon}(t)$. Fig. 5 (b) shows enlarged fragment of this area. The volumetric release of laser radiation in combination with the cooling effect of surface evaporation contributes to the formation of a temperature maximum at $T(x) \approx 0.9\,T_c$ = 6840 K at a depth of 14 nm (characteristic absorption length) and thus creates all the conditions for the development of explosive boiling. Accurate reproduction of the process of explosive boiling, which is a phase transition of a homogeneous type, within the continuum model is not possible. However, the results obtained show that the mechanism of explosive boiling in metals is the same as in weakly absorbing media and is associated with the formation of a near-surface temperature maximum.

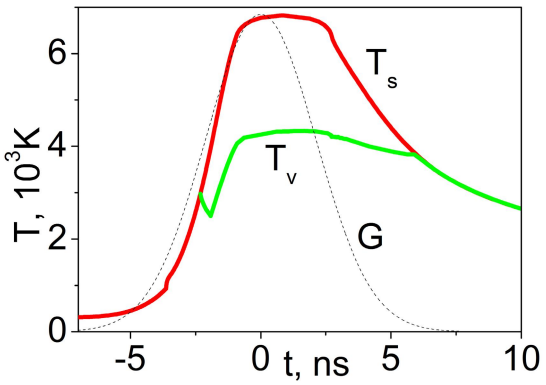

Fig. 1. Time profiles of surface (T_s) and vapor (T_v) temperature.

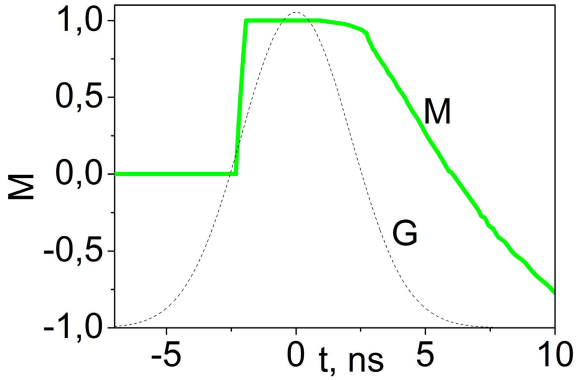

Fig. 2. Time profile of Mach number

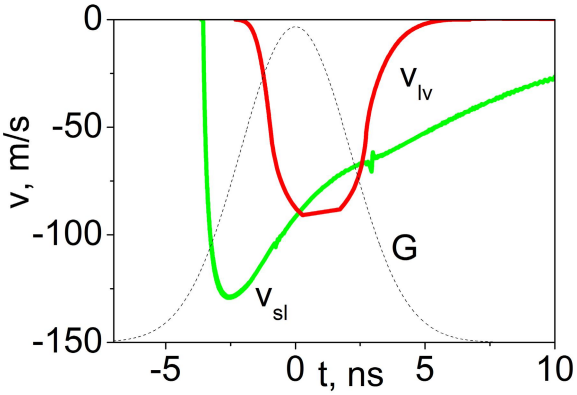

Fig. 3. Time profile of melting (v_{sl}) and evaporation (v_{lv}) velocity.

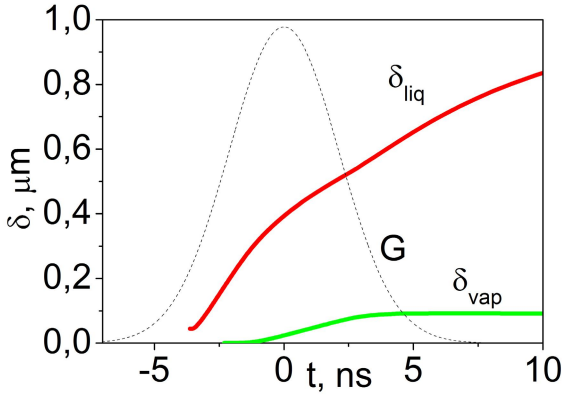

Fig. 4. Time profile of size of liquid (δ_{liq}) and vapor (δ_{vap}) (measured in corresponding amount of solid phase)

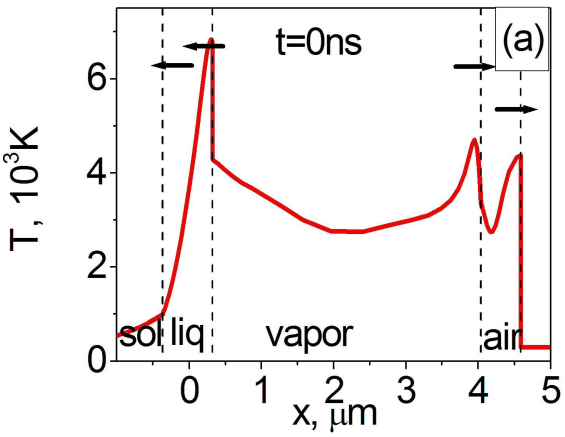

Fig. 5(a). Space profile of temperature at t=0.

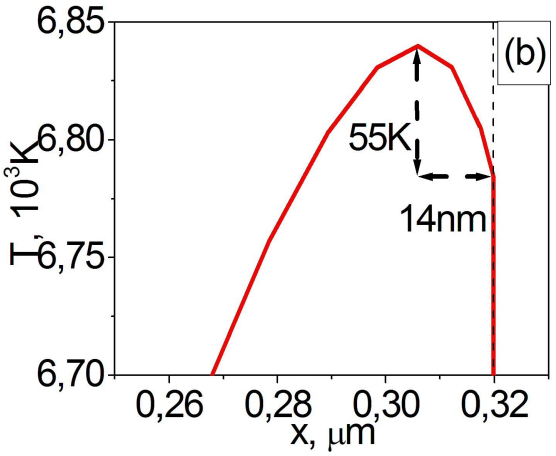

Fig. 5(b). Enlarged fragment of Fig. 5(a).

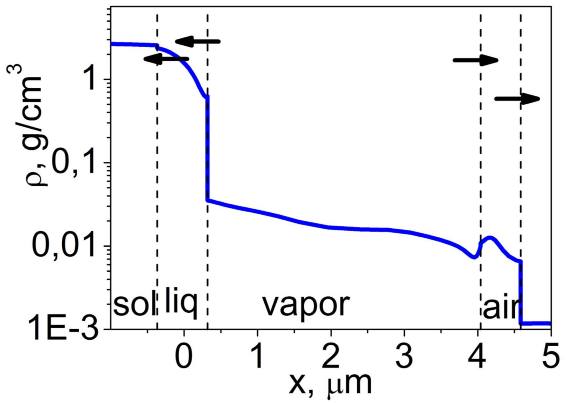

Fig. 6. Space profile of density at t=0.

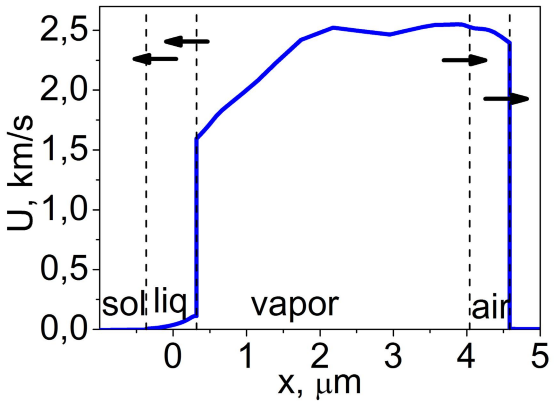

Fig. 7. Space profile of velocity at t=0.

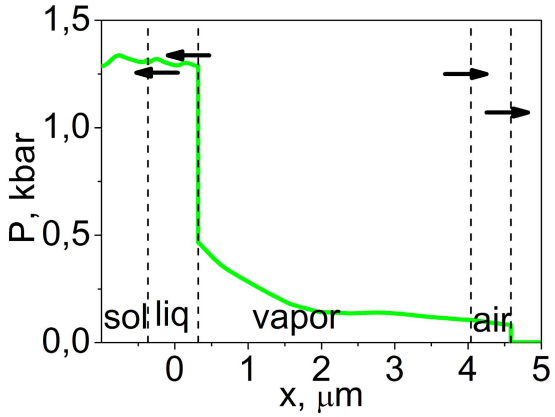

Fig. 8. Space profile of pressure at t=0.

3.1 Atomistic approach

Homogeneous mechanisms of phase transformations are characterized by the nucleation of a new phase in a certain volume of superheated/undercooled matter. Representing them in the continuum hydrodynamic models requires considerable additional efforts[19]. The most common and convenient, from the point of view of describing the kinetics of homogeneous phase transformations, are atomistic models[39] in which the classical or quantum equations of motion of a system of many particles, of which the sample under study is made, are solved numerically.

3.1.1 Homogeneous evaporation.

Molecular-dynamic modeling of the PLA process for greater visibility is performed with some simplifications. We used thin liquid Al film, with the sizes $X \times Y \times Z = 430 \times 6.2 \times 6.2\ nm$ (the total particle number $N = 5 \times 10^5$) with periodical boundary conditions in the directions $Y \times Z$, which heating was made in vacuum with constant laser intensity $G = 1.5 \times 10^8 Wcm^{-2}$ (absorbed intensity $G_s = 3.85 \times 10^7 Wcm^{-2}$). Laser radiation propagates from right to left and is normally incident on the free surface of the film. Part of the radiation is absorbed by the electronic components ($G_s = 3.85 \times 10^7 Wcm^{-2}$), and as a result of inelastic collisions is transferred to the ion subsystem. By using periodic boundary conditions in the directions Y, Z the problem is effectively reduced to one-dimensional approximation along the X direction (for transport processes of laser radiation and energy into electronic subsystem).
Combined TTM-MD model is used to describe the processes[40]. 3D molecular-dynamic modeling was used to describe the ion motion. At the initial time t = 0 the film was assumed to be heated to the temperature of 6340K, electron and ion subsystems are in thermal equilibrium.

The results of mathematical modeling show pulsed process consisting of five repeated explosive boiling processes at the time instants $t = 1.04,\ 1.44, 1.64,\ 2.0,\ 2.34\ ns$ while the laser duration was 3 ns. In Fig. 9, as an illustration, a snapshot of the third explosive boiling is shown.

The beginning of each explosive boiling was preceded by the formation of the temperature maximum in the film at the depth of $l \cong \kappa_L^{-1}$. Each time the separation of the fragment occurred at the point of the maximum. With each explosive boiling, the maximum values of temperature and pressure were significantly below the critical values: $T_{\max} \cong 7\,000\ K < T_c = 7\,600\ K$ и $p_{\max} < p_c = 1.42\ kbar$.

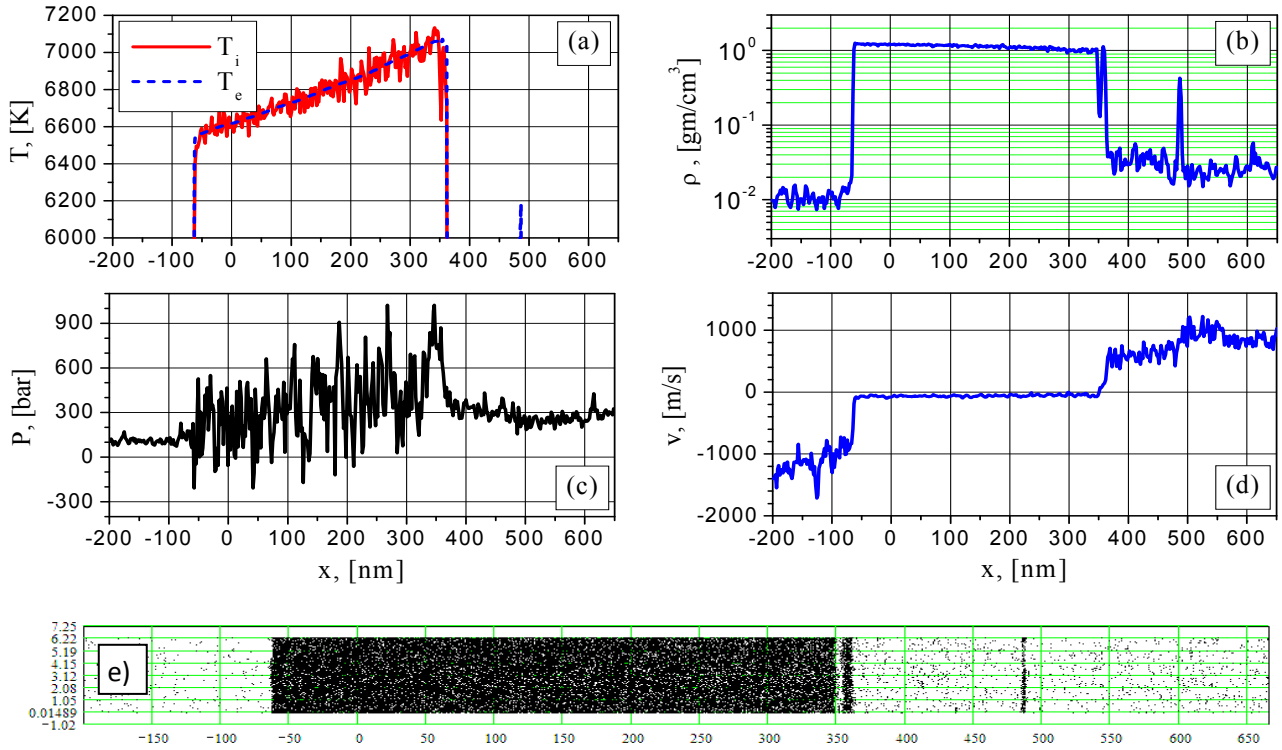

Fig. 9 Electron and ion temperature (a), density (b), pressure (c), velocity (d) and particle (e) distributions for I =38.5 MW/cm^2 at the time t =1.657 ns: third explosive boiling.

4. CONCLUSION

A continual hydrodynamic model has been developed that includes kinetic models of heterogeneous phase transitions-melting / crystallization and evaporation of metals.

With the help of continual and molecular dynamic modeling, the initial stage of a phase explosion in an Al target under the influence of laser ns radiation was investigated. The characteristic dimensions of the initial stage of explosive boiling, on which the formation of a region of vapor and a perturbed gaseous medium, of a limited shock wave is $\sim 5 \div 7\ \mu m$.

The results of the simulation showed that the phenomenon of spontaneous density fluctuations in a superheated metastable liquid in the vicinity of the critical point of matter with a maximum temperature below the surface is the basis of homogeneous evaporation (explosive boiling) of metals, resulting in the nucleation of a new phase.

The obtained results are in good qualitative agreement with the experimental data[16,17].

ACKNOWLEDGEMENTS

The research was funded by the Russian Scientific Foundation, grant No 15-11-30039.

REFERENCES

[1] Russo R.E., "Laser ablation," Appl. Spectrosc. 49, 14A– 28A (1995).
[2] Harilal S.S., Miloshevsky G.V., Diwakar P.K., LaHaye N.L., Hassanein A.. "Experimetal and computational study of complex shockwave dynamics in laser ablation plumes in argon atmosphere," Phys. Plasmas, 19, 083504 (2012).
[3] Farid N., Harilal S.S., Ding H., Hassanein A., "Emission features and expansion dynamics of nanosecond laser ablation plumes at different ambient pressures," J. Appl. Phys., 115(3), 033107 (2014)
[4] Benavides O., de la Cruz May L., Flores Gil A., Lugo Jimenez J.A., "Experimental study on reflection of high-intensity nanosecond Nd:YAG laser pulses in ablation of metals," Optics and Lasers in Engineering 68, 83–86 (2015).
[5] Hussein A. E., Diwakar P. K., Harilal S. S., and Hassanein A., "The role of laser wavelength on plasma generation and expansion of ablation plumes in air," J. Appl. Phys., 113, 143305 (2013)
[6] Phipps C.R., editor. [Laser ablation and its applications]. New York: Springer (2007)
[7] Gottfried J.L., De Lucia F.C., Munson C.A., Miziolek A.W., "Laser-induced breakdown spectroscopy for detection of explosives residues: a review of recent advances, challenges, and future prospects," Anal. Bioanal. Chem., 395, 283–30(2009).
[8] Cremers D. A. and Radziemski L. J., [Handbook of Laser-Induced Breakdown Spectroscopy], Wiley (2006).
[9] Hendow ST, Shakir SA. "Structuring materials with nanosecond laser pulses," Opt Express, 18, 10189–99 (2010).
[10] Al-Kattan A., Ryabchikov Y.V., Baati T., Chirvony V., Sánchez-Royo J. F., Sentis M., Braguer D., Timoshenko V.Yu., Anne Estève M. Kabashin A.V., "Ultrapure laser-synthesized Si nanoparticles with variable oxidation states for biomedical applications," J. Mater. Chem. B, 4, 7852-7858 (2016)
[11] Fadeeva E., Schlie-Wolter S., Chichkov B.N., Paasche G., Lenarz T., "Structuring of biomaterial surfaces with ultrashort pulsed laser radiation," Laser Surface Modification of Biomaterials, 145-172 (2016)
[12] Mazhukin V.I., Mazhukin A.V., Lobok M. G., "Comparison of Nano- and Femtosecond Laser Ablation of Aluminium," Laser Physics, 19, 5, 1169 – 1178 (2009).
[13] Mazhukin V.I., Nossov V.V., Smurov I., "Modeling of plasma-controlled surface evaporation and condensation of Al target under pulsed laser irradiation in the nanosecond regime," Appl. Surf. Sci., 253, 7686 – 7691 (2007).
[14] Li X.W., Wei W.F., Wu J., Jia S.L., Qiu A.C., "The influence of spot size on the expansion dynamics of nanosecond-laser-produced copper plasmas in atmosphere," J. Appl. Phys. 113, 243304 (2013).
[15] Lutey A.H.A., "An improved model for nanosecond pulsed laser ablation of metals," J. Appl. Phys., 114, 083108 (2013).
[16] Porneala C., Willis D.A., "Time-resolved dynamics of nanosecond laser-induced phase explosion," J. Phys. D: Appl. Phys., 42, 155503 (2009)
[17] Porneala C. and Willis D. A., "Effect of the dielectric transition on laser-induced phase explosion in metals", Int. J. of Heat and Mass Transfer, 49, 1928–1936 (2006)
[18] Xianfan Xu, "Phase explosion and its time lag in nanosecond laser ablation," Appl. Surf. Sci., 197–198, 61–66 (2002).
[19] Mazhukin V.I., Demin M.M., Shapranov A.V., "High-speed laser ablation of metal with pico- and subpicosecond pulses," Appl. Surf. Sci., 302, 6–10 (2014).
[20] Autrique D., Clair G., L'Hermite D., Alexiades V., Bogaerts A., and Rethfeld B., "The role of mass removal mechanisms in the onset of ns-laser induced plasma formation," J. Appl. Phys., 114, 023301 (2013)
[21] Dabby F., Paek U.C., "High-Intensity Laser-Induced Vaporization and Explosion of Solid Material," IEEE J.Quantum Electronics, 8 (2), 106 - 111 (1972).
[22] Bulgakova N. M. and Bulgakov A.V. "Pulsed laser ablation of solids: transition from normal vaporization to phase explosion," Appl. Phys. A, 73, 199 (2001)
[23] Kozlov B.M., Samokhin A.A., Uspenskii` A.B., "O chislennom analize pul`siruiushchego rezhima ispareniia kondensirovannogo veshchestva pod dei`stviem lazernogo izlucheniia", Kvantovaia e`lektronika», 2(9), 2061-2063 (1975)
[24] Miotello A., Kelly R., "Critical assessment of thermal models for laser sputtering at high fluences," Appl. Phys. Lett., 67 (24), 3535-3537 (1995).
[25] Jiang M. Q., Wei Y. P., Wilde G., Dai L. H., "Explosive boiling of a metallic glass superheated by nanosecond pulse laser ablation," Appl. Phys. Lett., 106, 021904 (2015).
[26] Mazzi A., Miotello A., "Simulation of phase explosion in the nanosecond laser ablation of aluminum," Journal of Colloid and Interface Science, 489, 1-5 (2016).
[27] Kelly R., Miotello A., "Comments on explosive mechanisms of laser sputtering," Appl. Surf. Sci., 96-98, 205-215 (1996)

[28] Mazhukin V.I., "Kinetics and Dynamics of Phase Transformations in Metals Under Action of Ultra-Short High-Power Laser Pulses", Chapter 8, In “Laser Pulses – Theory, Technology, and Applications”, Ed. by I. Peshko, InTech, Croatia, 219 -276 (2012).
[29] Jackson K.A, [The interface kinetics of crystal growth processes], 159–169 (2002).
[30] Mazhukin V. I., Shapranov A.V., Demin M.M., Kozlovskaya N.A, "Temperature Dependence of the Kinetics Rate of the Melting and Crystallization of Aluminum", Bulletin of the Lebedev Physics Institute, 43 (9), 283–286 (2016).
[31] Mazhukin V. I., Shapranov A.V., Perezhigin V.E., "Matematicheskoe modelirovanie teplofizicheskikh svoi`stv, protcessov nagreva i plavleniia metallov metodom molekuliarnoi` dinamiki", Mathematica Montisnigri, 24, 47 -65 (2012).
[32] Mazhukin V.I., Samokhin A.A., "Boundary conditions for gas-dynamical modeling of evaporation processes", Mathematica Montisnigri, 24, 8 - 17 (2012)
[33] Khight C.J., "Theoretical Modeling of Rapid Surface Vaporation with Back Pressure", ALAA J., 17(5), 81-86 (1979).
[34] Croat D., "An Application of Kinetic Theory to the Problems of Evaporation and Sublimation of Monoatimic Cases", J. Math. Phys., 15, 1-54 (1936).
[35] Mazhukin V.I., Demin M.M., Shapranov A.V., Smurov I., "The method of construction dynamically adapting grids for problems of unstable laminar combustion", Numerical Heat Transfer, Part B: Fundamentals, 44 (4), 387 - 415 (2003).
[36] Breslavsky P.V., Mazhukin V.I., "Dynamically Adapted Grids for Interacting Discontinuous Solutions", Computational Mathematics and Mathematical Physics, 47 (4), 687 – 706 (2007).
[37] Mazhukin V.I., Mazhukin A.V., Koroleva O.N., "Optical properties of electron Fermi-gas of metals at arbitrary temperature and frequency", Laser Physics, 19 (5), 1179 - 1186 (2009).
[38] Mazhukin V.I., Shapranov A.V., Samokhin A.A., Ivochkin A.Yu., "Mathematical modeling of non-equilibrium phase transition in rapidly heated thin liquid film", Mathematica Montisnigri, 27, 65 - 90 (2013).
[39] Zhigilei L.V., Lin Z. and Ivanov D.S., “Atomistic modeling of short pulse laser ablation of metals: connections between melting, spallation, and phase explosion”, J. Phys. Chem. C, 113, 11892-11906 (2009).
[40] Ivanov D.S., Zhigilei L.V., “Combined atomistic-continuum modeling of short-pulse laser melting and disintegration of metal films”, Phys.Rev.B, 68, 064114(1-22) (2003)